NASA Technical Memorandum 81345

An Analytical Investigation of the Free-Tip Rotor for Helicopters

Robert H. Stroub

February 1982

NASA
National Aeronautics and
Space Administration

NASA Technical Memorandum 81345

An Analytical Investigation of the Free-Tip Rotor for Helicopters

Robert H. Stroub, Ames Research Center, Moffett Field, California

NASA
National Aeronautics and
Space Administration

Ames Research Center
Moffett Field, California 94035

AN ANALYTICAL INVESTIGATION OF THE FREE-TIP ROTOR FOR HELICOPTERS

Robert H. Stroub
Aerospace Engineer
NASA-Ames Research Center
Moffett Field, California 94035

Abstract

A new rotor configuration called the Free-Tip Rotor was analytically investigated for its potential to improve helicopter forward-flight performance characteristics. This rotor differs from a conventional rotor only in the blade tip region. In this configuration, the tip is self-adjusting in pitch with respect to the rest of the blade, in accordance with a moment balance about its pitch axis. With this self-adjusting capability, the resulting pitch motion generates a more uniform airload distribution around the azimuth. Computer math models were used to compare performance characteristics of the Free-Tip Rotor with those of a conventional rotor operating at flight speeds from 130 to 160 knots. The results of this analysis indicate that the Free-Tip Rotor improves cruise L/DE by at least 22%.

NOMENCLATURE

b	number of blades
c	blade chord, m
Δc	free tip aerodynamic center offset from pitch axis, m
C_L	lift coefficient, $\frac{\text{lift}}{qs}$
$C_{L\alpha}$	Lift curve slope, $\frac{dC_L}{d\alpha}$, per rad
C_T/σ	rotor thrust coefficient, $\frac{\text{thrust}}{\rho bcR(\Omega R)^2}$
C_{mo}	pitching-moment coefficient, $\frac{\text{pitching moment}}{qSc}$
f	parasite drag area, $\frac{\text{drag}}{q}$, m^2
ℓ	distance from pitch axis to centrifugal force component, m
L/DE	$\frac{\text{rotor lift}}{\text{drag} + (\text{power}/V)}$
M	Mach number
$\overline{m}$	tip mass, kg
q	dynamic pressure, $(1/2)\ \rho V^2$, nt/m^2
R	blade radius, m
ΔR	free-tip radial length, m
S	reference area, m^2
V	airspeed, m/sec or knots
ρ	density of air, kg/m^3
Ω	rotor rotational speed, rad/sec
ω	free-tip pitch frequency, rad/sec
ϕ	inflow angle, $\tan^{-1}\frac{\text{velocities normal to disk plane}}{\text{velocities parallel to disk plane}}$
ψ	azimuthal angle, deg

Introduction

Because the tip has a strong influence on overall rotor performance and loads characteristics, the rotor blade-tip region has received considerable attention from aerodynamicists recently. To effect these characteristics, blade designers have generated numerous tip designs that have included one or more features, such as:

- planform shape variation including sweep
- dihedral variation
- twist variations
- offsets between the center of gravity and the aerodynamic center
- variations in structural coupling with inboard blade sections

Samples of how these design variables impact rotor performance are presented in (references 1 and 2). These references present an experimental evaluation of tip planform shapes that also included aerodynamic center offset from the elastic axis.

The tip design that is the subject of this report incorporates aerodynamic center offset from the pitch axis and center of gravity, and is free to pitch about its pitch axis. The tip design includes a structural coupling that does not pass torsional loads between the tip and the inboard portion of the blade, and a device that passively applies a constant external pitching moment to the tip. A tip designed with these features would be expected to produce a more uniform load distribution around the azimuth with a resulting improvement in rotor cruise L/DE and lessened oscillatory loads. This report presents the results of an analytical investigation of the Free-Tip Rotor and presents a performance comparison between a conventional and a Free-Tip Rotor at flight speeds of 130 to 160 knots.

The Free-Tip Rotor

The Free-Tip Rotor is a rotor with a tip having the following salient features:

1. The tip is free to rotate about its pitch axis and is decoupled from pitch motions of the inboard portion of the blade (figure 1).

2. The mass center of the tip is on its pitch axis which is located ahead or upstream of the aerodynamic center.

3. A controller that imparts a constant moment about the pitch axis of the tip so as to drive the tip nose up or to increase angle-of-attack. This pitching moment does not appreciably vary with pitch deflection.

With design features 1 and 2, the tip is free to pitch, or "weathervane" into the relative wind, tending to nullify any load perturbations that would

upset the moment balance about the pitch axis. That is, the tip functions like a simple weathervane trying to make the net pitching moment equal to zero but, as a consequence of the zero pitching moment, lift would be zero. The feature that makes the difference between the weathervane and the free tip configuration is design attribute 3, the controller. The controller applies a positive pitching moment to the tip which changes the angle of attack of the null point for the weathervaning action, thereby producing lift on the tip. The magnitude of the resulting lift is proportional to the magnitude of the controller applied moment, that is, for steady conditions:

$$\text{lift} \times \Delta\text{chord} = \text{controller applied moment}$$

where Δchord is the offset between the pitch axis and the aerodynamic center. Therefore, to modulate lift, it is merely necessary to modulate the controller applied moment. This arrangement consequently changes the lift control from the conventional position based system to a moment basis system. Note that the moment based system is the same lift control technique used by airplanes.

If the controller's applied moment is invariant with pitch angle of the tip and invariant with azimuth position, then there will be nearly constant lift as the blade traverses the azimuth. It is this natural tendency toward constant lift that is the major factor in achieving improved performance such as lower power required and higher L/DE. These improvements would result from reducing or eliminating negative lift on the advancing side while maintaining high lift on the retreating blade and elsewhere around the azimuth.

Because the free-tip functions on the basis of a moment balance around the pitch axis, the benefits of this tip configuration would be reduced if there are either significant time-variant pitching moments or moments that are not related to lift acting on the tip itself. Sources of time-variant aerodynamic moments would include compressibility, stall, and unsteady aerodynamics. Other potential sources of unwanted moments are inertial loads due to flapping and lead-lag motions. These motion induced moments could be detrimental because they reflect forces on the entire blade, not just the tip itself. In spite of these potentially degrading factors, a Free-Tip Rotor design can be shown to be effective in improving rotor performance.

The Math Model

To examine the potential of the Free-Tip Rotor, an existing state of the art math model was modified to represent the Free-Tip Rotor. This representation included the following modeling features:

1. Structural modeling - finite element modeling was used for flapwise and edgewise degrees of freedom, but the blade was torsionally rigid; flap and lag motions are fully coupled.

2. Downwash modeling - nonuniform downwash distribution based on a prescribed wake. The prescribed wake was developed from conventional rotor tip vortex only; it does not include any vortices shed from the junction of the tip and the inboard portion of the blade.

3. Aerodynamics - blade-element theory using airfoil lift, drag, and pitching-moment coefficients that include compressibility effects stall, unsteady effects and a 3-dimensional effect on compressibility drag at the tip. No aerodynamic drag penalty was applied to the junction between the free tip and the inboard portion of the blade.

4. Blade pitch angles - pitch angles for the free tip segment of the blade are based on the dynamic response to aerodynamic and inertial loadings using the response equations as developed below. For the blade elements inboard of the free tip, the pitch angles were prescribed around the azimuth using a steady and first harmonic representation.

The most significant limitations of this or any math model that affects its applicability to the free tip concept are the steady and unsteady aerodynamic characteristics of the tip and the aerodynamic environment the tip encounters. To date though, tip aerodynamics and its operating environment are not clearly known. However, since the objective herein is to investigate the Free-Tip Rotor configuration and not to investigate methodology per se, the inaccuracy and limitations of current technology were accepted and the basic unmodified math model was selected. The particular math model was selected because it included both steady and unsteady aerodynamics. It also included a prescribed, nonuniform wake structure; and it was in current use as a predictive tool. The basic math model was modified to reflect the tip's free pitching capability and the subsequent results where compared to those generated by the unmodified program. (Thus, the Free-Tip's payoffs were determined with both the free tip and the conventional tip having the same aerodynamic characteristics and with both tips operating in the same aerodynamic environment.

The free tip motion was modeled using its own equation of motion about the pitch axis:

$$I\ddot{\theta} + C\dot{\theta} + K\theta = M_{(t)}$$

where

θ, $\dot{\theta}$, $\ddot{\theta}$ = free-tip pitch angle and its first and second derivatives with respect to time measured relative to the rotor disk plane.

I = moment of inertia
C = aerodynamic damping
K = aerodynamic spring rate based on the product of lift curve slope and the aerodynamic center offset distance.

$M_{(t)}$ = external moment applied to the free tip including control moment, aerodynamic pitching moment, and inertial moments due to flapping and lag motions as functions of time.

If the system is assumed to be underdamped, the dynamic response to the equations of motion is given by the equations

$$\theta_{(to+\Delta t)} = \frac{M_{(to)}}{K} + \left[\theta_{(to)} - \frac{M_{(to)}}{K}\right] e^{-\Delta t(c/2I)} \times \cos(\omega\Delta t) + \left[\frac{2I\dot{\theta}_{(to)} + c\theta_{(to)}}{2I\omega} - \frac{M_{(to)}c}{2KI\omega}\right] e^{-\Delta t(c/2I)} \sin(\omega\Delta t)$$

$$\dot{\theta}_{(to+\Delta t)} = \dot{\theta}_{(to)} e^{-\Delta t(c/2I)} \cos(\omega\Delta t) - \left[\frac{2K\theta_{(to)} + c\dot{\theta}_{(to)}}{2I\omega} - \frac{M_{(to)}}{I\omega}\right] \times e^{-\Delta t(c/2I)} \sin(\omega\Delta t)$$

where:

to = time at origin or reference base for the subsequent motion
Δt = incremental time interval for a specified azimuthal interval
$\omega = \sqrt{4IK - C^2/2I}$, the damped, natural pitch frequency of the free tip.

These equations represent the dynamic response to a step function where the values for M, C, and K are expected to remain constant over the time interval Δt. At the end of time Δt, θ, and $\dot{\theta}$ values are combined with new values of C, K, and $M_{(t)}$ to become the initial conditions for the next azimuthal step. This process is repeated until a rotor revolution is completed and the θ at $\psi = 0$ equals (within a specified tolerance) its value on the previous revolution. The radial and azimuthal blade loadings are computed for the free tip and the inboard portion of the blade; the resultant blade motions determined; and then the whole process repeated until the rotor motions are stabilized.

Selection of Tip Parameters

The potential benefits of the Free-Tip concept may be assessed by comparing a conventional rotor to the same rotor with a free tip replacing the outboard section. Thus, the performance characteristics will be calculated for both the basic conventional rotor and the Free-Tip Rotor. Cruise power requirements and L/DE will then be compared.

The geometry of the hypothetical conventional rotor is as follows:

R = 7.77m	twist = 8°
c = .4764m	solidity = 0.078
ΩR = 214.6m/sec	number of blades = 4

The airfoil sections are VR-7 from root cutout to 0.9R and VR-8 from 0.9R to tip. Aerodynamic characteristics of the VR-7 and VR-8 airfoils are presented in figure 2.

Flapwise and edgewise elastic properties and mass distributions are presented in figure 3.

For this investigation, the free tip consists of the outer 6% of the blade which is considered a practical choice. The selection was somewhat arbitrary, but optimization of this and other design parameters is beyond the scope of this report.

The remaining geometric parameters of the free tip are determined by desired natural-frequency characteristics and desired inertial couplings. A high "aerodynamic spring" rate, $C_{L_\alpha} \Delta c(qc\Delta R)$, and a low pitch inertia will generate the high aerodynamic natural frequency that will give the free tip the greatest weathervaning potential to minimize lift perturbations around the azimuth. The center of gravity will be made coincident with the pitch axis which is located at the .13 chord position to minimize unwanted inertial coupling effects. With the center of gravity and the pitch axis both at the .13 chord line, and using advanced materials technology, a pitch inertia of 7.38×10^{-4} kg m sec^2 is felt to be feasible. The free tip is torsionally decoupled form the inboard portion of the blade; hence, there is assumed no elastic spring to affect the aerodynamic spring.

The following values were used for the five free tip design parameters; however, they may be considered as independent parameters:

1. Center of gravity at 0.13 chord station
2. Pitch axis at 0.13 chord station
3. Moment of inertia of 7.38×10^{-4} kg m sec^2
4. A tip span equal to 6% of the radius or .465m
5. The VR-8 tip airfoil.

The undamped natural frequency is calculated using:

$$\omega = \sqrt{\frac{\text{aerodynamic spring rate}}{\text{pitch inertia}}}$$

$$= \sqrt{\frac{\rho V_T^2 C_{L\alpha} \Delta c (\Delta R) c}{2I}}$$

With the above independent design parameters, the chosen chord length and a $C_{L\alpha}$ = 5.73 per rad., this becomes

$$\omega = 2.58\ V_T$$

for

$$V_T = \Omega R \left(1 + \frac{V}{\Omega R} \sin \psi\right),$$

thus,

$$\omega = 554 \left(1 + \frac{V}{\Omega R} \sin \psi\right)$$

or

$$\frac{\omega}{\Omega} = 20.05 \left(1 + \frac{V}{\Omega R} \sin \psi\right)$$

With this magnitude of aerodynamic natural frequency, the free-tip will follow high frequency flow perturbations, and have a high potential for achieving improved performance.

The final item to be designed is the controller, which applies a pitching moment to the free tip. The controller moment could be steady, oscillatory, or some combination of the two. The control moment time and azimuthal characteristics will be the result of a particular controller design selected. Since there are numerous possible designs, which utilize one or more energy sources, a treatise on various controller designs is beyond the scope of this report. For this investigation, the selected controller design is a simplified version of the design depicted in reference 3. This design was simplified by eliminating the pilot's ability to modulate the control moment; therefore, the controller only produces a specified moment level that is invariant with time, azimuth and pitch angle. The controller pitching moment, M_c is generated in this manner: centripetal acceleration, $\Omega^2 R$, acting upon the tip mass, $\bar{m}$, which is free to move along a helical path that is wrapped around the pitch axis and makes an angle γ with a plane normal to the pitch axis. The resulting centrifugal force component along the helical path, $\bar{m}\Omega^2 R \sin \gamma$, acts at distance ℓ from the pitch axis thus creating the controller moment. For computational purposes, the controller pitching moment about the spar pitch axis is mathematically expressed as

$$M_c = \ell \bar{m} \Omega^2 R \tan \gamma$$

Figure 4 presents a pictorial view of how controller moment is created. In this figure, note that motion along the helical path also creates pitch angle θ for the tip. Since there is no mechanical spring in this controller configuration, the generated pitching moment would not be sensitive to the difference in pitch angles between the tip and the inboard portion of the blade. To sum up, the controller moment would be insensitive to azimuth position and would be insensitive to differential pitch angles and would be set at a specified moment level. The controller moment setting will be determined by the free tip lift requirement to achieve a desired hovering performance. The relationship between the lift coefficient and the controller moment is developed below, based on moment balance about the pitch axis.

(controller moment) + (aerodynamic moment) + (structural moment)

+ (inertial moments) = 0

$$(M_c) + \left(C_{mo} - C_L \frac{\Delta c}{c}\right) c^2 \Delta R \frac{\rho}{2}(\Omega R) + (M_{ST}) + (\Sigma M_I) = 0$$

For this free tip design, the tip is torsionally decoupled (no mechanical spring) from the remaining part of the blade, consequently $M_{ST} = 0$. Since the center of gravity is on the pitch axis, the major inertial moments vanish leaving less significant moments which are $I\Omega^2\theta$ and the tennis racket moment. The sum of these two terms is .2 nt-m of nose down moment. It remains only to select C_L and C_{mo}. Selecting a design C_L of .4 based on a desired hover performance and selecting a section C_{mo} of +0.02, the resulting required controller moment is 1.5 nt-m.

Cruise Performance Comparison

The effect of the Free-Tip concept on cruise performance will be evaluated by a side-by-side comparison between the conventional rotor and the Free-Tip Rotor; each generating the same thrust, the same propulsive force and the same trimmed hub moments at the same forward speed. The selected nominal thrust was 60940 nt corresponding to a C_T/σ of 0.073. The rotors provided sufficient propulsive force to overcome a parasite drag area of 1.25 m^2 corresponding to a f/bcR value of 0.085, a value representive of a modern "clean" helicopter. At these thrust and propulsive force values, the Free-Tip Rotor required significantly less power. In figure 5 the Free-Tip Rotor required 11% less power than the conventional rotor at 160 knots and 24% less power at 130 knots. These lower power requirements can be transformed into greater lift and payload carrying capability, higher maximum speed, greater cruise efficiency, or combinations thereof. The power improvements in terms of cruise efficiency are shown in figure 6 where the Free Tip concept enables cruise L/DE gains of 18% at 160 knots to 40% at 130 knots. Compared to a conventional rotor, the Free-Tip concept is effective in reducing power requirements in forward flight and in markedly improving cruise efficiency.

The improved efficiency of the Free-Tip Rotor accrues from two basic phenomena. First, the free tip itself is generating more steady lift than the conventional rotor tip. This is significant because, if both rotors are producing the same thrust and propulsive forces, then the inboard portion of the

blade must be generating less lift. This is depicted in figures 7 and 8 which presents mean inplane thrust and mean drag resolved into the shaft axis system for the 160 knot forward flight case. In figure 7, the free tip portion of the blade is seen to generate 756 nt more lift than the tip of the conventional rotor, while conversely, the conventional rotor is generating more steady lift inboard. With more steady lift inboard, those inboard blade stations experience greater profile drag and a larger induced drag penalty $C_L \sin \phi$.

For flight speeds between 160 knots and 130 knots, the inboard lift distributions of the two rotor configurations are similar to the 160 knot case shown. The primary differences are in the oscillatory peak values of tip lift. At 130 knots, the free tip generated 1068 nt of lift which is 312 nt more lift than at 160 knots. With more tip lift at 130 knots, the inboard stations had to generate proportionally less lift which consequently resulted in more power saving at 130 knots than at 160 knots.

Another mechanism by which the free tip reduced the need for shaft driving power is through lower drag coefficients on the advancing blade tip region. The tip of a conventional rotor experienced high drag because it carried negative lift on the advancing portion of the disk. (The negative lift was the result of accumulated longitudinal cyclic requirements and blade twist.) The Free Tip, however, did not carry negative lift. This is illustrated in figures 9 and 10 which present the lift and drag coefficients for a representative tip station at 160 knots. It is seen that the free tip does not experience negative lift and the corresponding high drag coefficients in the critical region around $\psi = 90°$. In contrast to the conventional rotor, the free tip is at zero lift which is also minimum drag. Thus, the free-tip concept is seen to reduce power requirements by eliminating the usual negative lift region on the advancing tip. This, in turn, reduces the high transonic drag in this area.

In the above discussion, it was pointed out that the free tip generates higher average lift than the conventional tip configuration. This characteristic is inherent to the concept and occurs naturally with this configuration. This is because the free tip will generate a smoother, less oscillatory lift distribution around the azimuth, with a mean level determined by a sufficiently high applied control moment. In this application of the free tip concept, lift smoothening resulted all around the azimuth, but the major impact was in the advancing blade region where the free tip reduced the lift drop off. A key concept characteristic is that higher average tip lift can occur even though the free tip did not go to lift levels higher than the peak levels of the conventional tip. This is shown in figure 11 which presents the instantaneous aerodynamic normal force of the tip for both rotors at 160 knots. The free tip did not generate the large negative lift at $\psi = 90°$ which is characteristic of conventional rotors. Also, the free tip did not generate a higher instantaneous maximum lift level (lift measured from the zero airload line) than the conventional tip; in fact, the free tip instantaneous maximum lift levels were lower and it still produced a higher mean lift level. Also, note the more rapid rise in airload after $\psi = 100°$ with the free tip. After $\psi = 100°$, the free tip is seen striving to generate the desired lift level over the remaining azimuthal travel with a resulting smoother, less oscillatory lift distribution at a higher mean lift level. Thus, the Free Tip can and does achieve greater steady lift without exceeding retreating blade C_L limits. At the same time, it achieves a side benefit of reduced power required.

It was also mentioned previously that the lift on the free tip was less at 160 knots than at 130 knots. This reduction with forward speed is the result of changes in pitching moment brought about by higher advancing tip Mach number. The advancing tip Mach number affected the pitching moment in the following way. As the tip Mach number progressed beyond 0.71, the aerodynamic pitching moment coefficient decreased toward more negative values. This negative increment in pitching moment coefficient, operating on a higher dynamic pressure, resulted in a reduction in the net positive pitching moment about the pitch axis and therefore less lift. This effect is depicted in figure 12 where aerodynamic normal force is presented for the 0.955 radial station for both 130 knots and 160 knots. The product of C_m and dynamic pressure, which is directly proportional to $C_m M^2$, is shown for both speeds at $\psi = 90°$ of the two effects, a more negative C_m or a greater dynamic pressure, the largest contributor was the negative shift in C_m by about 2 to 1. Notice that after the azimuthal zone of the sharp reduction in lift ($20 < \psi > 140$), tip lift returns to about the same levels. Thus, even though the free tip is operating at a high Mach number (21% greater than the Mach number for moment break for this airfoil), it is still able to achieve better performance than the conventional rotor.

With the free tip pitching independently of the inboard portion of the blade, there will be a pitch angle difference between the blade and free tip. This is shown in figures 13a and 13b for the 130 knot and 160 knot conditions. As may be seen in these figures, the largest differences in pitch are about 2° and 3.0°, occurring in the general vicinity of $\psi = 80°$ and $\psi = 325°$, respectively. Any performance penalty arising from the discontinuity due to pitch angle differences will depend on how the intersection is configured. A radial transition zone would be best since the pitch angle differences would be spread over a finite spanwise length rather than a step. Therefore, for that case, lift losses and drag penalties would be minimized. Certainly, any gap that would leak pressure between the upper and lower surfaces could cause high drag and be undesirable. Sealing the gap against air leakage may be an important design requirement for this concept to be successful. With modern materials, solutions to the problems of sealing the gap and eliminating the discontinuity appear to be within easy reach.

Summary and Conclusions

The results of this study have shown that analytically, the Free Tip Rotor is effective in reducing cruise horsepower by 11% at 160 knots. This improvement was the result of change in rotor spanwise lift distribution decreasing both profile and induced power of the entire rotor. The free tip was able to carry more lift than the conventional rotor tip because the free tip smoothed the azimuthal distribution of airloads, especially around $\psi = 90°$. In that sector, the free tip airload did not go negative, whereas the conventional blade tip did go deep into negative lift with the accompanying high drag. The free tip was shown to have a sensitivity to transonic pitching moment characteristics which can degrade the performance gains. These characteristics can be overcome in future designs with sweep, for example. The

pitch angle differential was found to be less than ± 3° for the speed range investigated. The gap or step between the free tip and the inboard blade could be configured in future designs to minimize a potential drag penalty.

The results presented herein are from math models with known limitations that are applicable to the conventional rotor configuration as well as applicable to the Free-Tip Rotor. Therefore, an experimental investigation of the FreeTip Rotor is the next logical step to corroborate the findings from the math model and to demonstrate the feasibility of the concept. Such a test program has in fact been initiated.

REFERENCES

1. Stroub, R.H., Rabbott, J.P., and Niebanch, C.F.; "Rotor Blade Tip Shape Effects on Performance and Control Loads from Full-Scale Wind Tunnel Testing", Journal of the American Helicopter Society, Vol. 24, No. 5, October 1979.

2. Blackwell, R.H., Murrill, R.J., Yeager, W.T., Mirick, P.H.; "Wind Tunnel Evaluation of Aeroelastically Conformable Rotors", paper presented at the 36th Annual National Forum of the American Helicopter Society, May 1980.

3. Stroub, R.H.; United States Patent, "Constant Lift Rotor For a Heavier Than Aircraft", No. 4,137.010, January 30, 1979.

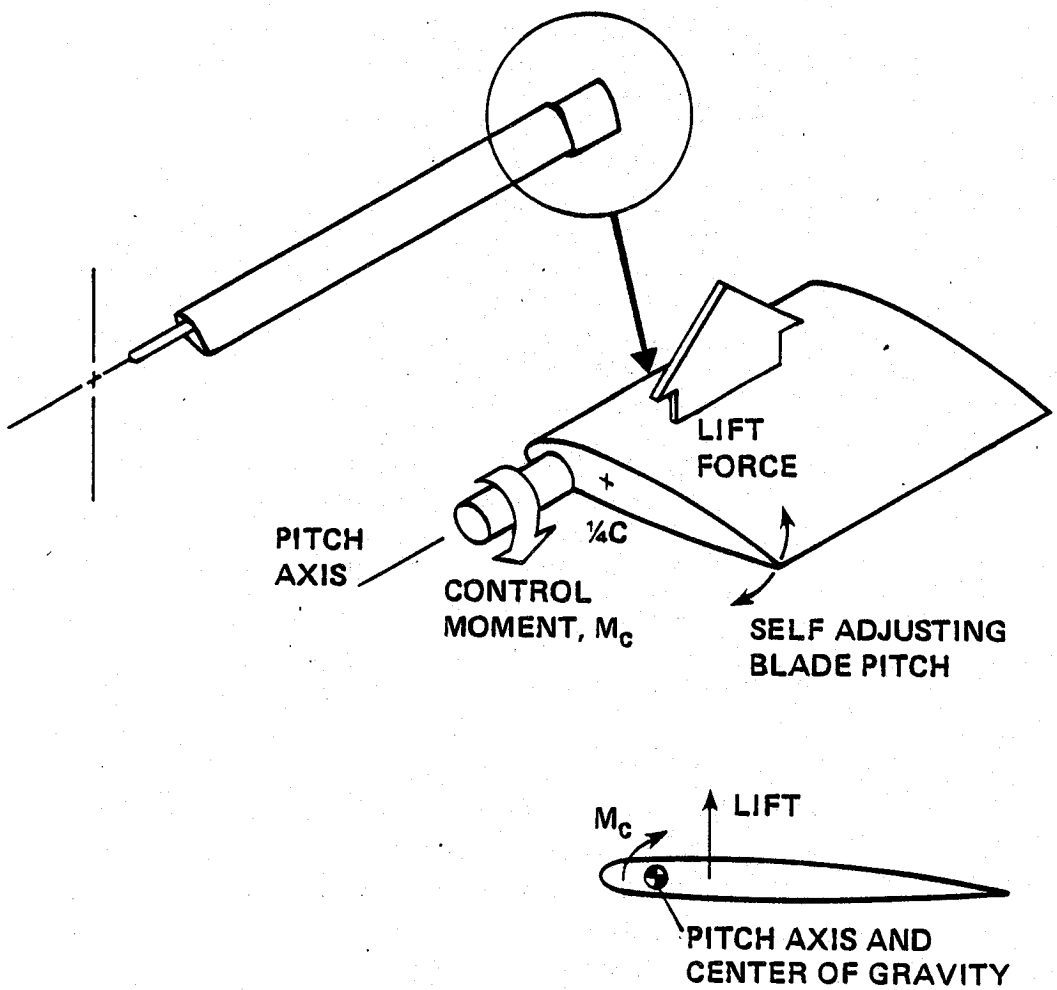

Figure 1. The Free-Tip rotor schematic.

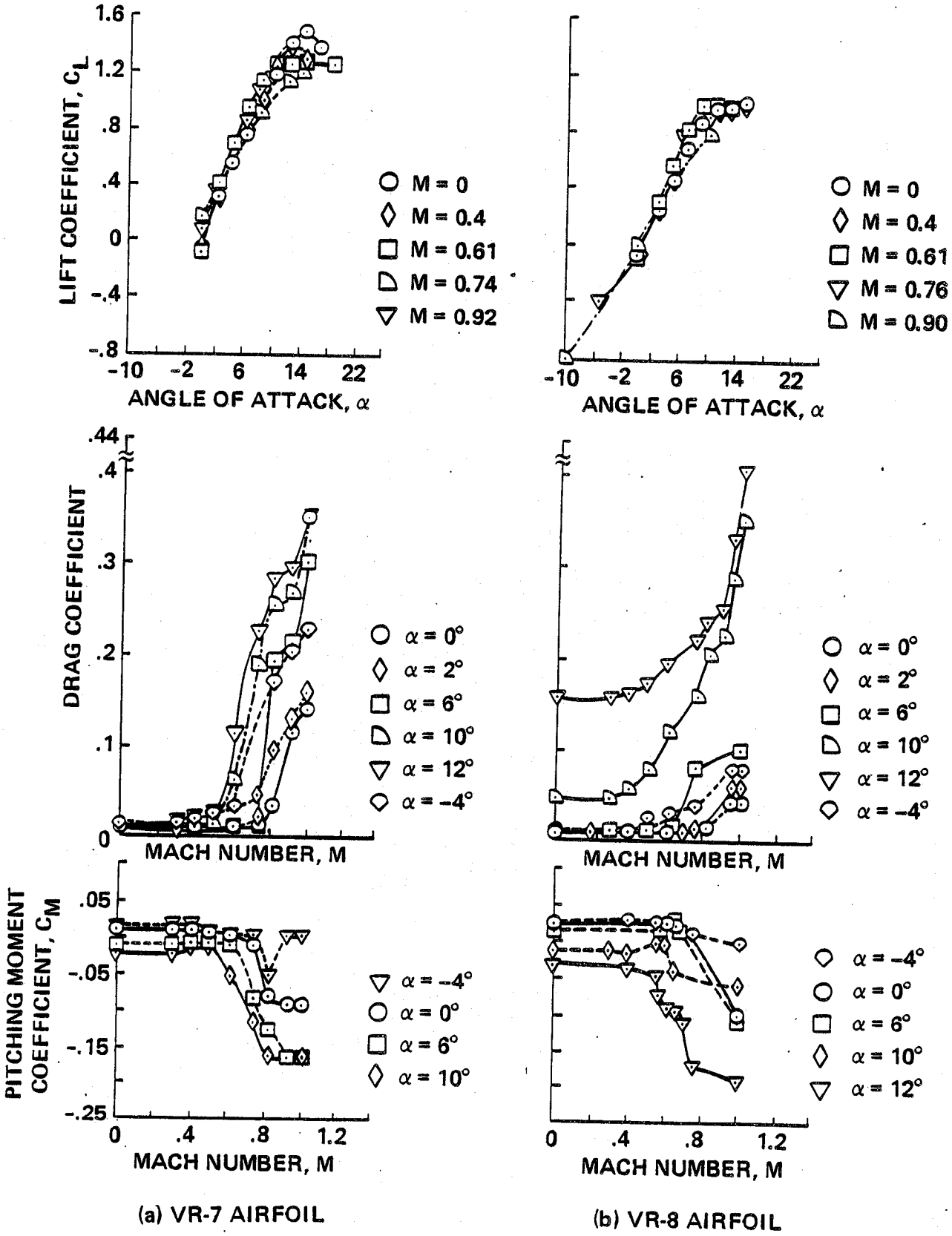

(a) VR-7 AIRFOIL

(b) VR-8 AIRFOIL

Figure 2. Aerodynamic characteristics of the VR-7 and VR-8 airfoil.

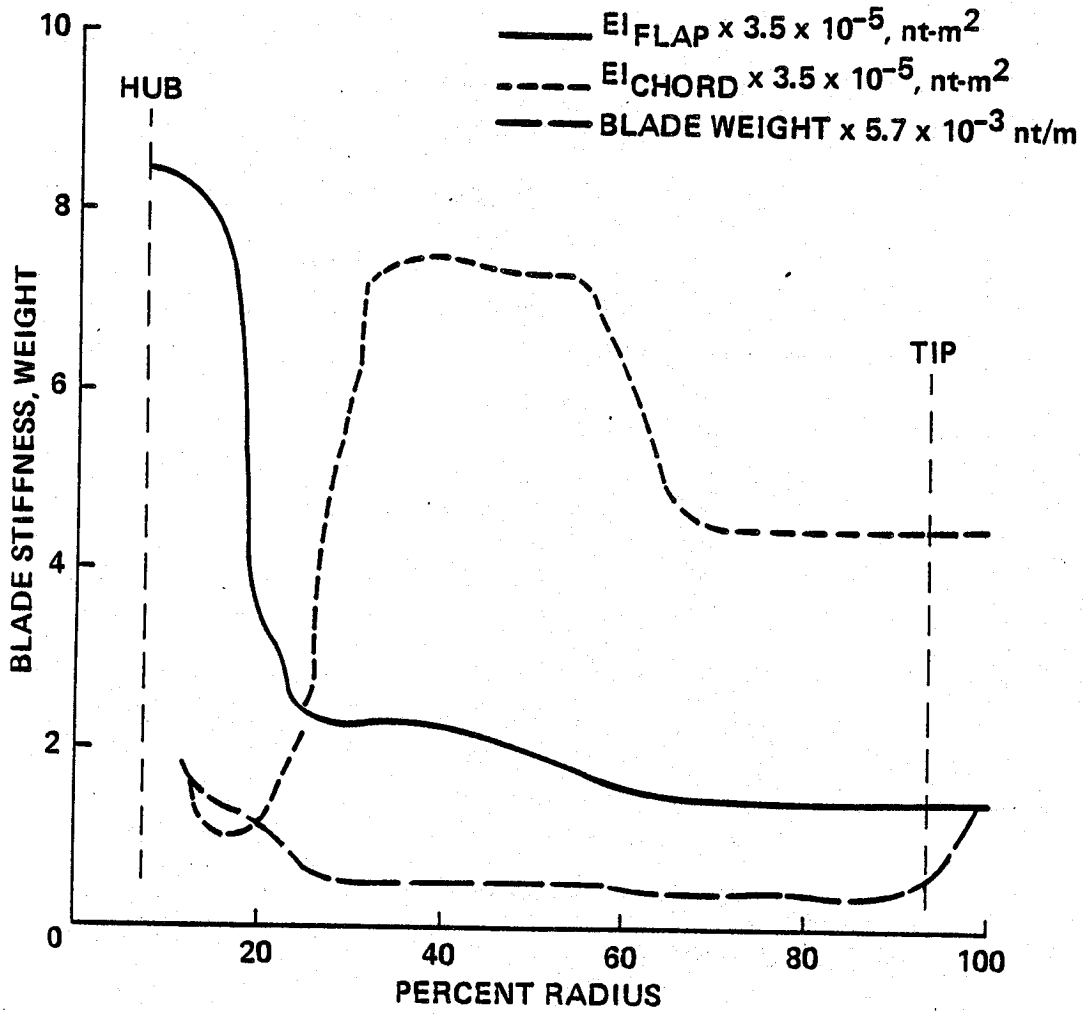

Figure 3. Mass and structural stiffness properties for the conventional rotor and for the Free-Tip rotor.

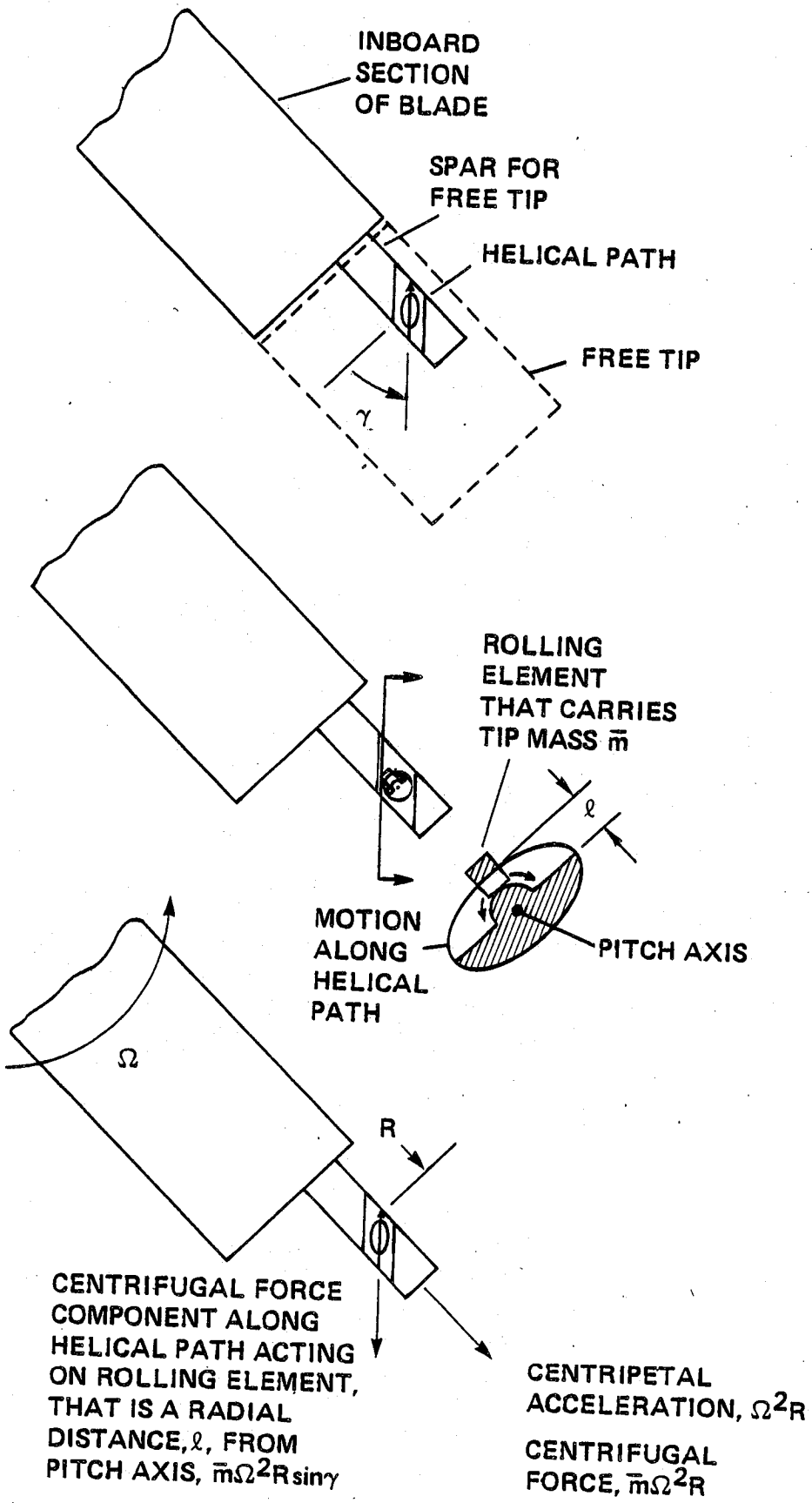

Figure 4. Creation of Pitching Moment by Controller

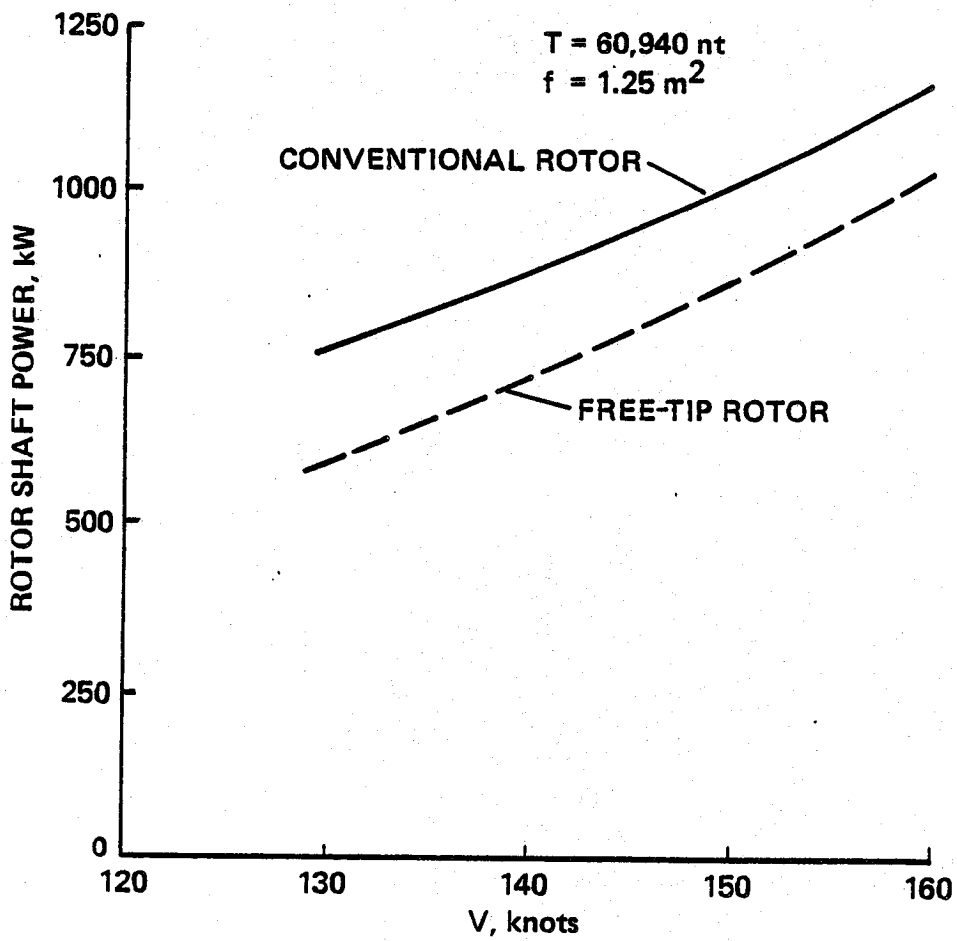

Figure 5. Comparison of speed-power characteristics at sea level, standard conditions.

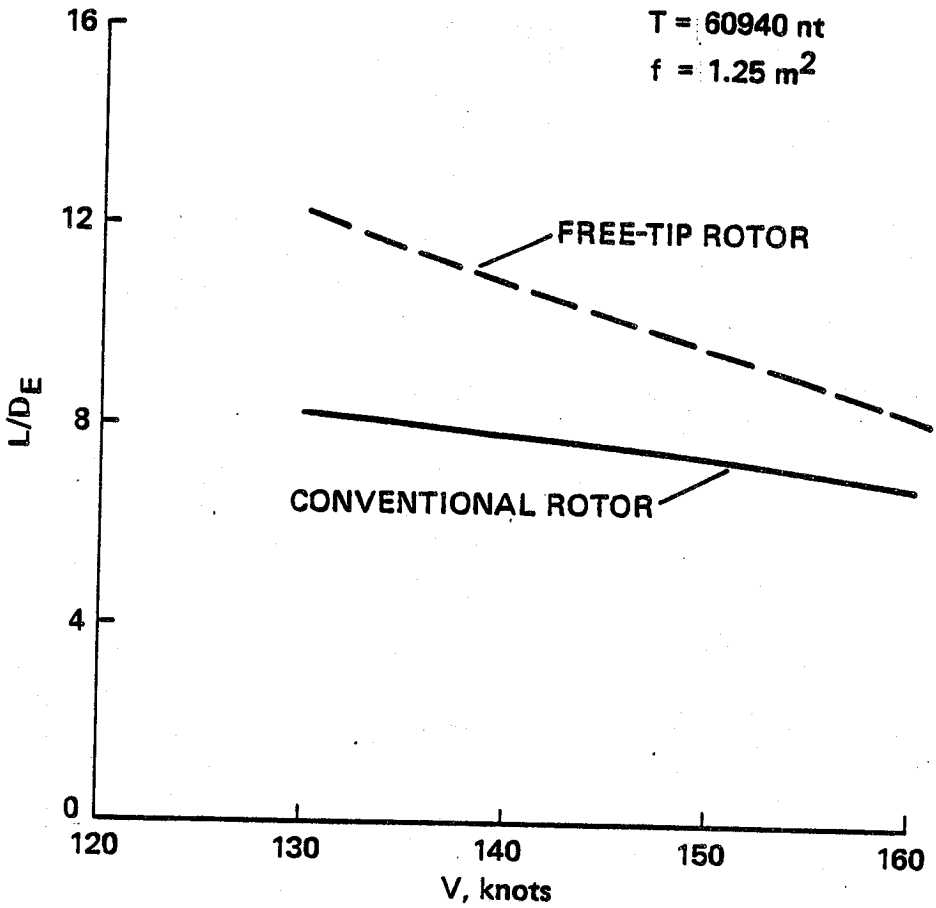

Figure 6. Cruise efficiency comparison between conventional and Free-Tip rotor.

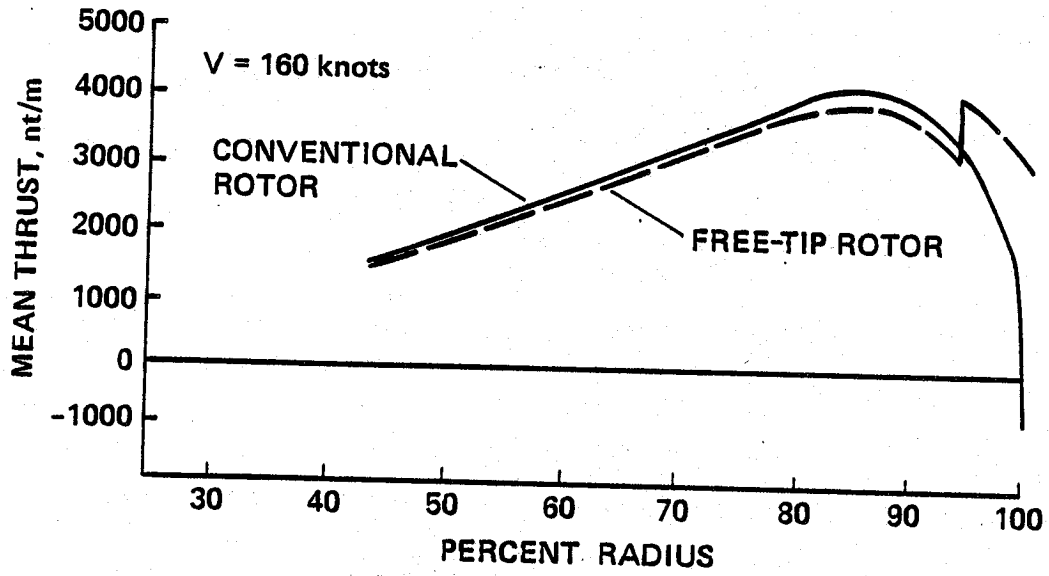

Figure 7. Mean thrust loading at V = 160 knots for thrust = 60940 nt.

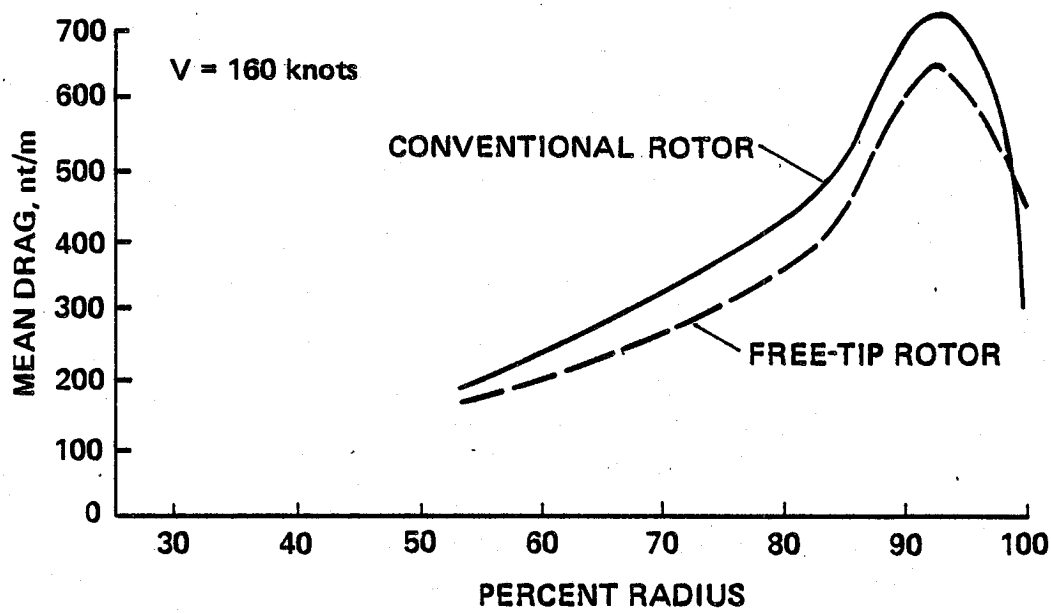

Figure 8. Mean inplane drag loading at V = 160 knots for thrust = 60940 nt.

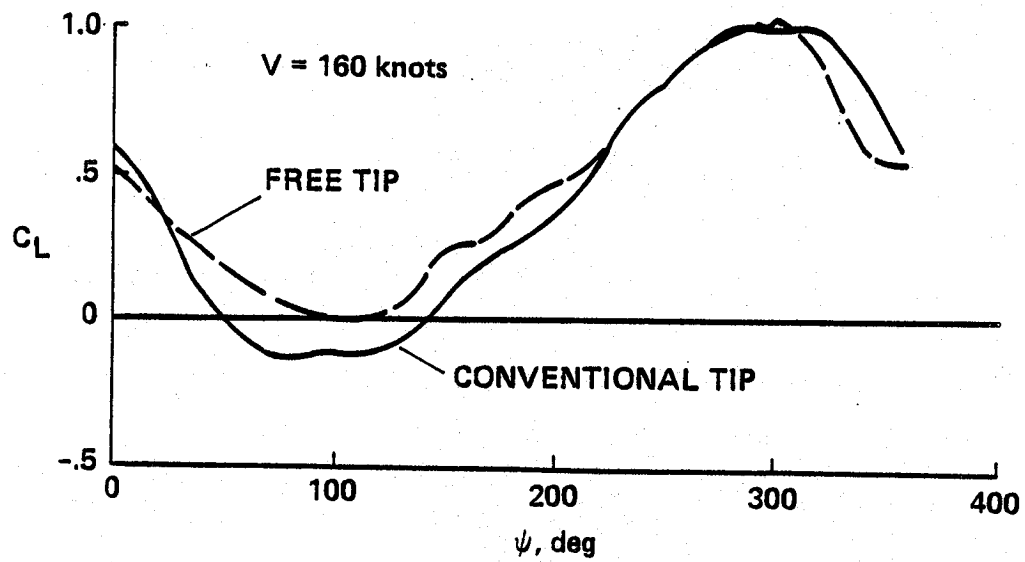

Figure 9. Instantaneous lift coefficients at the 0.955 radial station for thrust = 60940 nt.

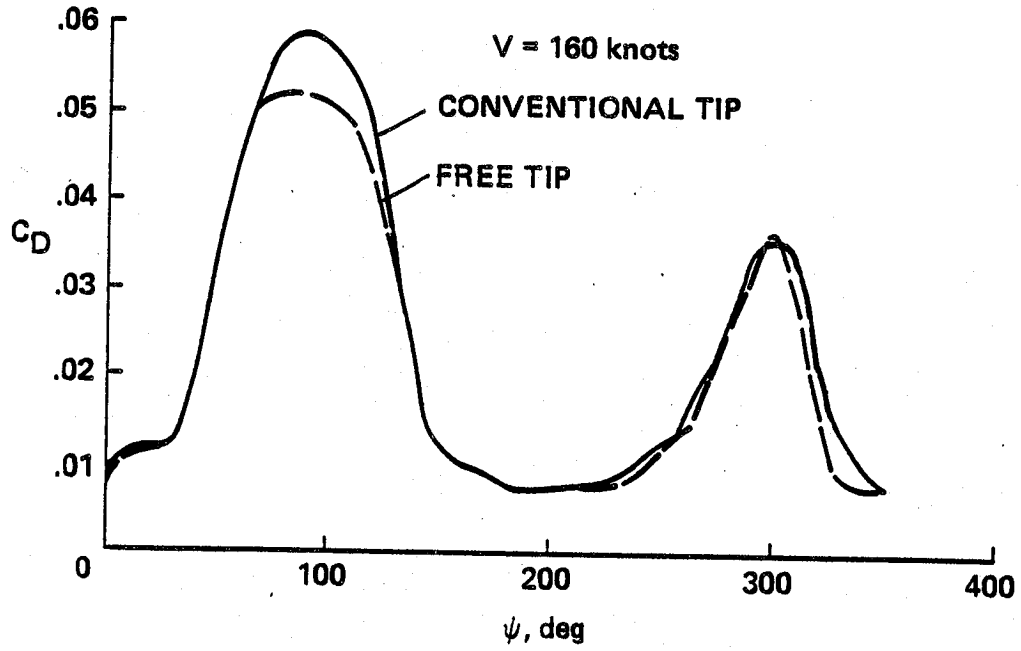

Figure 10. Instantaneous drag coefficients at the 0.955 radial station for thrust = 60940 nt.

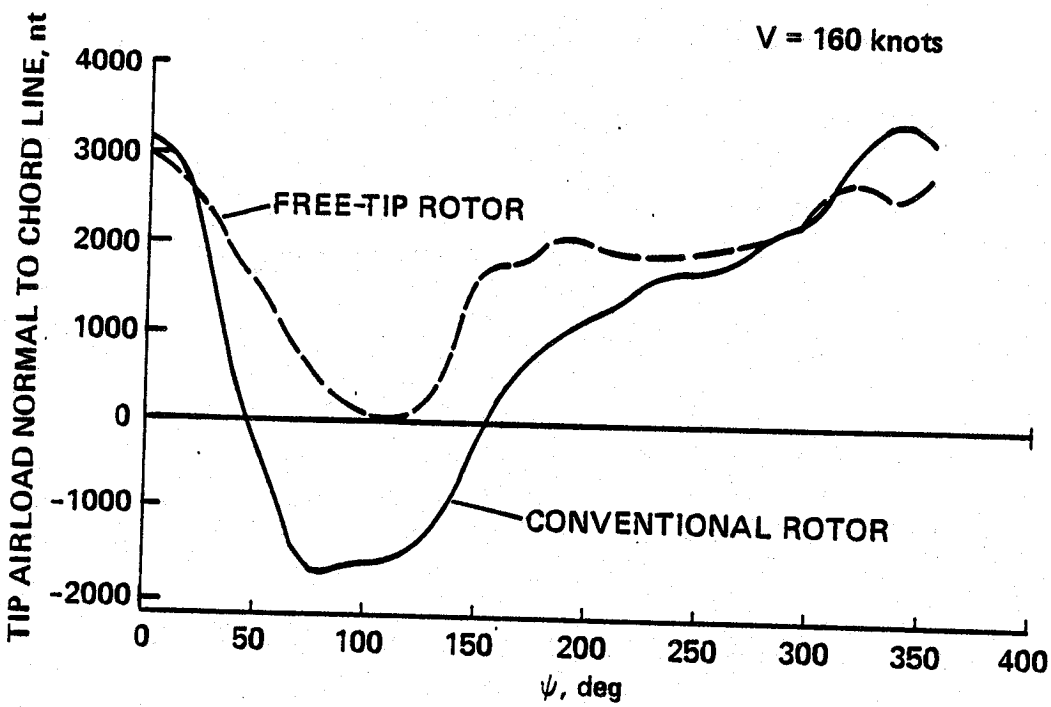

Figure 11. Azimuthal variation of tip airload at 160 knots and 60940 nt thrust.

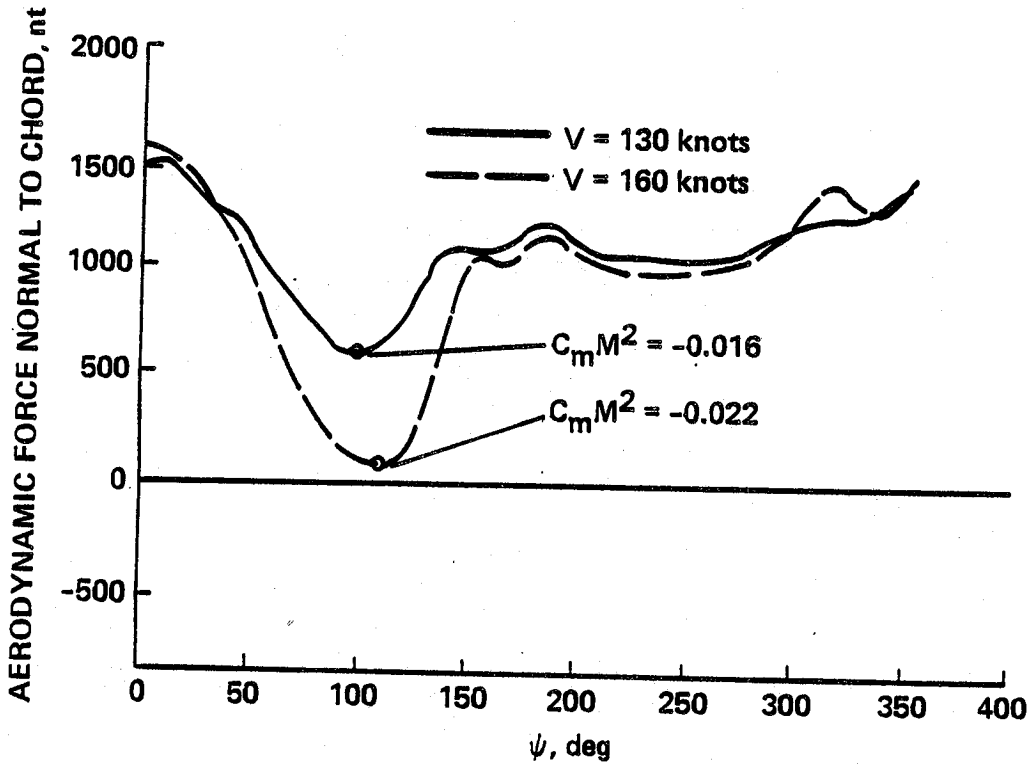

Figure 12. Normal force characteristics at the .955 radial station of the free tip at 130 knots and 160 knots.

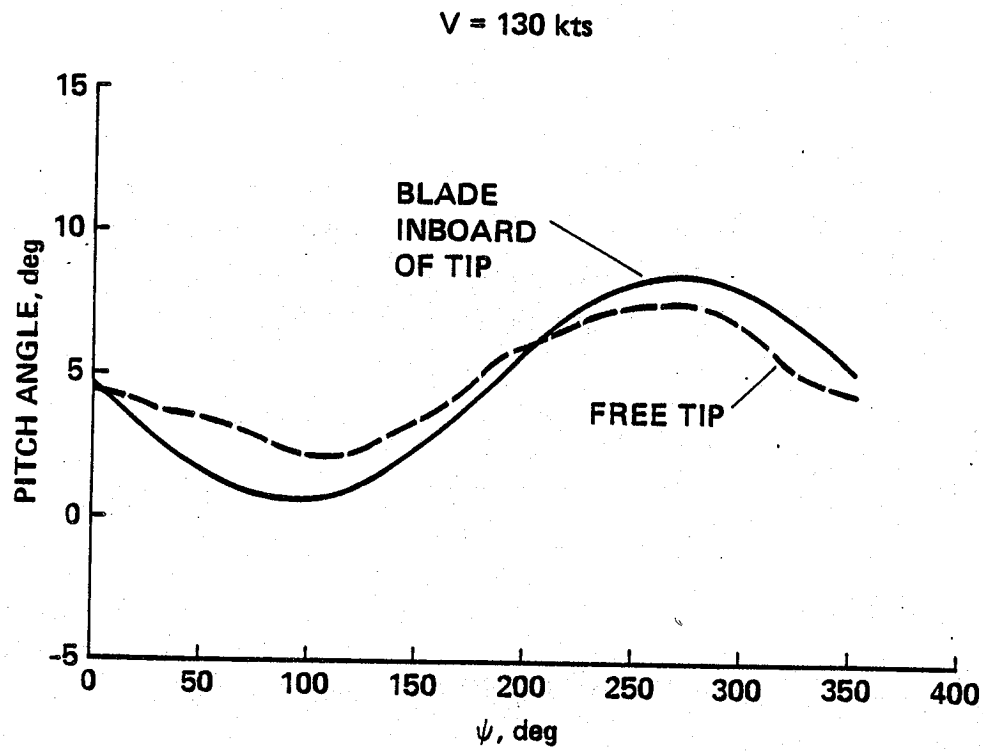

Figure 13a. Pitch angle discontinuity between Free Tip and inboard portion of blade; V = 130 knots.

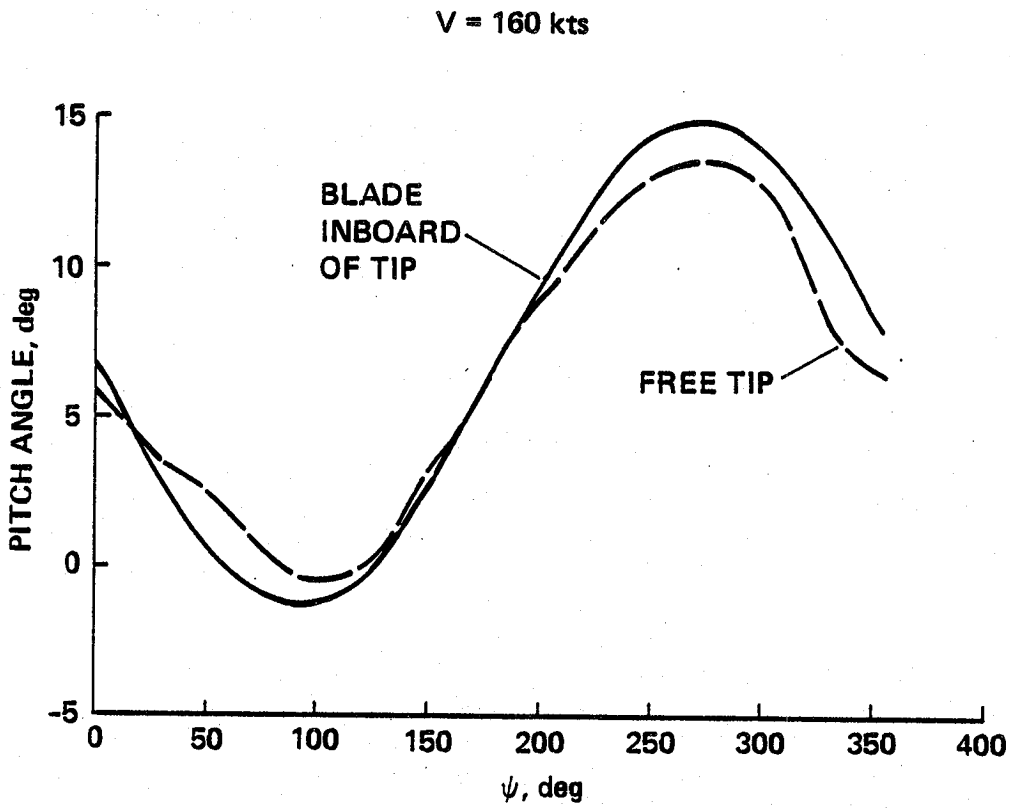

Figure 13b. Pitch angle discontinuity between Free Tip and inboard portion of blade; V = 160 knots.

1. Report No.	2. Government Accession No.	3. Recipient's Catalog No.
NASA TM		

4. Title and Subtitle	5. Report Date
AN ANALYTICAL INVESTIGATION OF THE FREE-TIP ROTOR FOR HELICOPTERS	February 1982
	6. Performing Organization Code
7. Author(s)	8. Performing Organization Report No.
Robert H. Stroub	A-8806
9. Performing Organization Name and Address	10. Work Unit No.
Ames Research Center, NASA Moffett Field, Calif. 94035	532-03-11
	11. Contract or Grant No.
12. Sponsoring Agency Name and Address	13. Type of Report and Period Covered
National Aeronautics and Space Administration Washington, D.C. 20546	Technical Memorandum
	14. Sponsoring Agency Code

15. Supplementary Notes

Point of Contact: Robert H. Stroub, Mail Stop 247-1, Moffett Field, Calif. 94035 FTS 448-965-6653, (415) 965-6653.

16. Abstract

A new rotor configuration called the Free-Tip Rotor was analytically investigated for its potential to improve helicopter forward-flight performance characteristics. This rotor differs from a conventional rotor only in the blade tip region. In this configuration, the tip is self-adjusting in pitch with respect to the rest of the blade, in accordance with a moment balance about its pitch axis. With this self-adjusting capability, the resulting pitch motion generates a more uniform airload distribution around the azimuth. Computer math models were used to compare performance characteristics of the Free-Tip Rotor with those of a conventional rotor operating at flight speeds from 130 to 160 knots. The results of this analysis indicate that the Free-Tip Rotor improves cruise L/DE by at least 22%.

17. Key Words (Suggested by Author(s))	18. Distribution Statement
Rotor tips Free floating tips Helicopter performance Rotor characteristics	Unlimited STAR Category - 02

19. Security Classif. (of this report)	20. Security Classif. (of this page)	21. No. of Pages	22. Price*
Unclassified	Unclassified	16	A01

*For sale by the National Technical Information Service, Springfield, Virginia 22161